Hydrol. Earth Syst. Sci. Discuss., 9, 9455–9501, 2012
www.hydrol-earth-syst-sci-discuss.net/9/9455/2012/
doi:10.5194/hessd-9-9455-2012

Hydrology and Earth System Sciences Discussions

Discussion Paper | Discussion Paper | Discussion Paper | Discussion Paper |

Snow glacier melt estimation in tropical Andean glaciers using Artificial Neural Networks

V. Moya Quiroga, A. Mano, Y. Asaoka, and K. Udo

Graduate School of Engineering, Tohoku University, Sendai, Japan

Received: 12 July 2012 – Accepted: 31 July 2012 – Published: 13 August 2012

Correspondence to: V. Moya Quiroga (moyav@potential1.civil.tohoku.ac.jp)

Published by Copernicus Publications on behalf of the European Geosciences Union.

Abstract

Snow and glacier melt (SGM) estimation plays an important role in water resources management. Although melting process can be modelled by energy balance methods, such studies require detailed data which is rarely available. Hence, new and simpler approaches are needed for SGM estimations. Artificial Neural Networks (ANN) is a modelling paradigm able to reproduce complex non-linear processes without the need of an explicit representation. The present study aims at developing an ANN based technique for estimating SGM rates using available and easy to obtain data such as Temperature and short wave radiation. Several ANN models were developed to represent the SGM process of a tropical glacier in the Bolivian Andes. The main data consisted on short wave radiation and temperature. It was found that accuracy may be increased by considering relative humidity and melting from previous time steps. The model represents the daily pattern showing variation of the melting rates throughout the day, with highest rate at noon. The melting rate in October (1.35 mm h^{-1}) is nearly three times higher than July's melting rate (0.50 mm h^{-1}). Results indicate that the exposure time to melting in October is 12 h, while in July is 9 h. This new methodology allows estimation of SGM at different hours throughout the day, reflecting its daily variation which is very important for tropical glaciers where the daily variation is greater than the yearly one. This methodology will provide useful data for better understanding the glacier retreat process and for analysing future water scenarios.

1 Introduction

Any human activity relates somehow to water, but unfortunately it is not a renewable resource. Although more than 70 % of the planet is covered by water, most of it is saline water from the oceans. Glaciers could be considered as the most important water reservoirs, since they represent about 68 % of the total fresh water available (Shiklomanov and Roda, 2003). SGM is of outmost interest for different water related areas like water supply, sediment transport, flood forecasting or as reservoirs storing water as ice and releasing it when melted (Jansson et al., 2003), but most of them are located in the poles far from human activities; only mountainous glaciers are located in human populated continental areas. Mountainous glaciers could be considered the world's virtual water towers assuring year round water flow for the main rivers, and its melting may lead to water shortage for millions of people. Unfortunately, most of the mountain glaciers are melting quite rapidly, fact that may lead to serious social tensions related to water. Hence, it is important to understand glacier dynamics in order to analyse possible future water scenarios.

There have been many studies about glaciers and snowfall, both at global and local scales. Radic and Hock (2010) applied a statistical method to estimate global glacier volume and states that corresponds to a sea level equivalent of 0.7 m. Hirabayashi et al. (2008) analysed global snowfall distribution from 1959 to 2006 and found a decrease in snowfall after the mid 1980s. Henneman and Steffan (1999) found seasonal variations in albedo for snow and ice in the Minessota region. Avian and Bauer (2006) monitored Pasterze glacier with laser scanning technique and detected three zones of collapsing ice body. Huss et al. (2010) analysed the spatial distribution of Switzerland glaciers by relating glacier surface elevation change as a response of mass balance change. Asaoka and Kominami (Asaoka, 2012) reconstructed snowfall distribution in Japan by combining a snow model with remote sensing data. Koboltsching and Schoner (2011) investigated the contribution of glacier melt to total river run off in the Austrian Alps. Also different measures to prevent melting like covers, water injection or snow compaction were tested at field locations (Olefs and Fischer, 2008). Nevertheless, the above mentioned studies were applied to high latitude locations where climatic conditions are different than tropical latitude places like the Andes.

Dynamic of the tropical Andes is quite different than Alpine Glaciers; while the Alps experience a long accumulation period in winter, the Andes experience permanent ablation throughout the year (Coudrain et al., 2005). The tropical Andean glaciers used to cover over 2940 km^2, but suffered a strong retreat that decreased its area to 2493 km^2

HESSD
9, 9455–9501, 2012

by 2002 and caused some small glaciers such as Chacaltaya or Cotacahi to disappear (Vergara et al., 2007), with serious consequences. For instance, the area around Cotocachi not only experienced decrease in agriculture and tourism activities but also more and worse water conflicts are expected over time. Important Bolivian cities such as La Paz and Cochabamba already faced serious social tensions categorised as emblematic in global water debates (Laurie and Crespo, 2007). Thus, a better water resources management (WRM) is an important goal. Simulation modelling became a key tool for achieving such goal, since they allow making predictions under different scenarios. Hence, SGM simulation is an important and necessary tool.

There are different analytical methods for simulating glacier melt like nomographs, temperature index models and energy based models. Nomographs (Ambach, 1986) not only are a manual and time consuming option, but also specific nomographs have to be developed for a given case; thus, they could be considered as a derivative of the other two methods. Although temperature index models are a simplification of complex process that would be better described by energy balance, many studies found high correlation between melt and air temperatures (Hock, 2003). Temperature models relate the amount of melting to a degree day factor and to either the sum of the positive temperature or the mean daily temperature. Sometimes temperature index models use a base temperature that might be below the freezing temperature (Debele et al., 2009). Since they have the advantage that temperature is an easy to measure data, they are popular and used in many studies (Hock, 1999; Jost et al., 2012; Biggs and Whitaker, 2012). Nowadays, some hydrological models like HEC-HMS or MikeSHE include the option of snow/ice melting by using temperature based equations (Abbott et al., 1986; Scharffenberg and Fleming, 2010). One of the most popular temperature models is the Snow-Melt Run off Model (SRM) designed to simulate and forecast daily stream flow in mountain basins and used in different places (Wang et al., 2010; Tahir et al., 2011; Bocchiola et al., 2011). Hirabayashi et al. (2010) estimated global glacier mass balance using the global glacier model HYOGA that uses a day degree approach. Nevertheless,

HESSD
9, 9455–9501, 2012

such model cannot simulate the temporal variation in South American glaciers due to the scarce data.

However, earlier studies showed that just air temperature is not enough for predicting snow melt (Zuzel and Cox, 1975). It is important to consider that temperature of matter is just a property that represents the relation between the heat added to a body and its change in entropy (King, 2005), thus the external heat added to a given body (in this case radiation) is the external force that defines the matter property. Besides, all the temperature models have a minimum time scale of daily estimations and the conceptual limitation that energy available for melt is not linearly related to positive air temperatures (Hock and Holmgren, 1996). Therefore, they are not able to reproduce daily pattern fluctuations which are important in tropical regions. Moreover, Khun (1987) showed that melting may happen at air temperatures as low as $-10\,^{\circ}$C. Hence, radiation must be included in melting models.

Energy balance melt models are based upon the assumption that at freezing temperature any surplus of energy at the surface air interface will be used for melting, and the energy available for melting is then related to the latent heat of fusion. Basic energy balance models were applied to simulate snow melt in Nordic glaciers (Hock and Holmgren, 2005), in the Alps (Sicart et al., 2008), New Zealand (Anderson et al., 2010) and in the Andes (Sicart et al., 2011). The extended approach that combines global radiation and temperature was implemented to the WaSiM-ETH model (Schulla and Jasper, 2007) and applied to alpine river basins (Verbunt et al., 2003). There are also more advanced energy models that divide the snowpack into layers and then apply a 1-D mass and energy balance to each layer in order to predict temperature profiles. The 1-D energy balance model SNTHERM was applied to analyse the variation of soil temperature with snow cover and improving roads maintenance (Fu et al., 2009). The land surface model ISBA-ES was coupled to models SAFRAN (meteorological model) and MODCOU (hydrogeological model) to simulate spring and summer flows in the French Alps (Lafaysse et al., 2011). However, above mentioned models face the main limitation of detailed data requirements which is difficult to obtain, and sometimes it can be obtained only for limited periods of time. Hence, new alternatives are needed to estimate glacier melting with more accessible data.

ANN are mathematical structures able to represent complex non-linear relationships between input and output by imitating functioning of neurons in a human brain. In the last years, ANN have been successfully applied in hydrological studies. They were used for sediment studies (Kisi et al., 2012), weather forecast downscaling (Hoai et al., 2011), rainfall forecasting (Hung et al., 2009), river flow estimations (Dai et al., 2009; Akhtar et al., 2009; Shamseldin, 2010; Huo et al., 2012), litoral drift predictions (Singh et al., 2008), estimate evapotranspiration (Cobaner, 2011). Other studies used them for modelling moisture fluxes (Neal et al., 2011). Although widely applied to hydrology, almost no studies applied ANN to snow and glaciated areas. Yilmaz et al. (2011) applied ANN to estimate flow in a snow dominated mountainous basin in Turkey, but its time step was limited to daily scale and the model was not able to reproduce the yearly pattern. That model was developed as a seasonal model.

The present study developed different ANN models to estimate instantaneous glacier melt rate in the Bolivian Andes using available and easy to obtain data. This research is not only among the first ones to estimate SGM at short time step without complex data, but also among the first ones to implement ANN technologies in tropical glaciers in an undeveloped country. The results will allow to easily predicting future SGM at any time according to different climate change scenarios. One main contribution of the present study is that it will allow overcoming the problem of data scarcity.

2 Study area

The Condoriri and Zongo glaciers are both within the Capricorn tropic in the Bolivian Andes at some 13 km from each other (Fig. 1).

The area has a marked seasonality of precipitation and cloud cover with wet season coincident with the austral summer (November–March), and dry season in winter (April–September) (Sicart et al., 2005). This pattern may be observed when analysing the solar radiation (Fig. 2). The short wave radiation has maximum values in winter due to the clear skies, while during summer it has lower values due to the cloudiness that attenuate it. On the other side, long wave radiation has lower values in winter and higher values in summer due to the radiation reflected by clouds. The temperature reaches its highest values in summer and lowest values in winter; but due to the high altitude it is common to have frozen temperatures even in summer. It can be said that the daily variation is greater than the seasonal one, which is typical behaviour of tropical latitudes (Mote and Kaser, 2007).

The Zongo Glacier with altitudes ranging from 4900 to 6000 m above the sea level (m a.s.l.) is located in the Huayna massif (16°16′ S, 68°10′ W) and is part of a 3.7 km^2 basin with the main limnimetric station at 4830 m a.s.l. (Sicart et al., 2007). It is located some 30 km north of La Paz. This glacier is being monitored since 2003 with the Zongo-ORE meteorological station within the project GLACIOCLIM (Glaciers un Observatorie du Climat). Unfortunately, the latest data available is from 2009, and there are some long data gaps of several months.

The Condoriri Glacier with altitudes from 4400 to 5200 m a.s.l. (16°11′ S, 68°13′ W) has the shape of a condor with open wings and provides water for the 70 % of El Alto and La Paz. In Condorir glacier along with Huayna and Tuni glaciers are currently being studied under the JICA's financed GRANDE (Glacier Retreat Adaptation for National policy and DEvelopment) project that will allow researchers to comprehend what's happening to the glaciers and to predict future scenarios. One major problem of the above mentioned glaciers is the lack of data. In July 2011 GRANDE project installed weather stations around the mentioned glaciers. Although the stations will provide current data at small time intervals, the measured parameters are not enough to perform a complete energy budget.

HESSD
9, 9455–9501, 2012

3 Data and methods

3.1 Data

Data for the Zongo Glacier was obtained from ORE-Zongo meteorological station installed and monitored by the French project GLACIOCLIM (http://www-lgge.ujf-grenoble.fr/ServiceObs/). This station has a data logger Campbell-ORE23x. It records every 30 min several meteorological parameters such as: short wave radiation, long wave radiation, temperature, relative humidity, wind speed and wind direction. The complete data base consists of nearly 78 000 time series data covering the years 2003–2009. However, there are some data gaps at different periods, especially in the first year. Besides, the GLACIOCLIM project estimates the yearly glacier melt by glaciological measurements (Perroy et al., 2007). Until the year 2004 the glacier fluctuation was estimated by averaging the initial and final glacier edge. Then, a new methodology was adopted by comparing the initial and final area based on a given reference line. Such estimations were used for the validation of the model.

Data for the Condoriri Glacier was obtained from the Condoriri weather station installed by the GRANDE project (http://grande.civil.tohoku.ac.jp/index_e.html). This station installed in July 2011 has a data logger HOBO-U30 that records every 10 min several meteorological parameters like short wave solar radiation, wind velocity, relative humidity, temperature and rain. The present study used more than 17 600 time series data from July 2011 to November 2011. This is an important period, since it is the season change from winter to spring.

3.2 Energy model

The estimation of SGM by energy methods is based on the assumption that once the glacier reached freezing temperature any surplus of energy is used for melting (Hock and Holmgren, 2005). The method may be applied either at single locations or over distributed models involving computations over a grid covering the study area. The current energy available for melt is estimated as the residual of the energy balance for each time step Eq. (1).

$$Q_M = SW_{in} + LW_{in} + SW_{out} + LW_{out} + Q_H + Q_L + Q_O \quad (1)$$

where

- Q_M = energy flux available for melting,
- SW_{in} = incoming short wave radiation flux,
- LW_{in} = incoming long wave radiation flux,
- SW_{out} = outgoing short wave radiation flux,
- LW_{out} = outgoing long wave radiation flux,
- Q_H = sensible heat flux,
- Q_L = latent heat flux,
- Q_O = other heat fluxes.

Usually radiation is measured at the site. Sometimes it may be estimated by a valid relation considering the location (latitude and longitude), the Julian day, possible cloudiness and time exposed to solar radiation which is influenced by the local topography. In the present study, both LW and SW radiation were obtained from Zongo station.

Sensible heat is calculated as function of the wind speed and temperature (Eq. 2):

$$Q_H = C_p k^2 \frac{\rho P u (T - T_f)}{P_o \ln(Z/Z_{ow}) \ln(Z/Z_{ot})} \quad (2)$$

where

- C_p = specific heat air at constant pressure,

HESSD
9, 9455–9501, 2012
Snow glacier melt estimation in tropical Andean glaciers
V. Moya Quiroga et al.

- k = Von Karman constant,
- P = atmospheric pressure,
- u = wind speed,
- P_o = standard atmospheric pressure,
- Z = instrument height,
- Z_{ow} = roughness for wind logarithmic profile,
- Z_{ot} = roughness for temperature logarithmic profile,
- T_f = freezing temperature,
- P = air density.

Latent heat is calculated as function of the wind speed and humidity (Eq. 3):

$$Q_L = 0.623 L k^2 \frac{\rho u(e_2 - e_o)}{P_o \ln(Z/Z_{ow}) \ln(Z/Z_{oe})} \quad (3)$$

where

- L = latent heat flux of evaporation,
- e_2 = vapour pressure at 2 m,
- e_o = vapour pressure at melting surface,
- Z_{oe} = roughness parameter for vapour pressure logarithmic profile.

HESSD
9, 9455–9501, 2012
Snow glacier melt estimation in tropical Andean glaciers
V. Moya Quiroga et al.

The other energy fluxes were neglected, since they represent a minimum percentage of the total. Then, the energy available for melt is converted into its water equivalent by relating to the water latent heat of fusion (Eq. 4).

$$\mathrm{WE} = \frac{Q_\mathrm{M}}{L_\mathrm{f}} \tag{4}$$

where

- WE = Water equivalent ($\mathrm{mm\,s^{-1}\,m^2}$),
- L_f = Water latent heat flux of fusion.

Hock and Holmgren (1996) suggested roughness values for glacier areas of Z_ow = 0.0027 m, Z_ot = 0.000027 m, Z_oe = 0.000027 m. Sicart et al. (2011) studied the Zongo Glacier and suggest a value of Z_ow ranging from 1 to 10 mm and $Z_\mathrm{ot} = Z_\mathrm{oe} = Z_\mathrm{ow}/100$, while other studies consider them as calibrating variables. Sicart et al. (2005) found that both latent and heat fluxes in Zongo are small and they play a minor role in the total energy balance since radiation supplies most of the melting energy. Also Van As (2011) found that solar is the main source of melting energy, and the errors of assuming constant roughness's are negligible. Thus, it can be assumed that the uncertainties of considering constant roughness values are small and without much influence. Other heat sources such as rain are too low that may be neglected.

SGM was estimated by applying the energy model with data obtained from the Zongo-ORE station. Every time step (30 min) energy balance was calculated. Then it was compared with previous time step SGM in order to consider the possible refreezing effect. In case energy balance was negative, it was assumed as freezing (Hock and Holmgren, 2005) and the next time step energy must compensate such freezing before allowing for melting. Once there was enough energy for melting, such energy was related to the latent heat of fusion for water which was assumed 33 400 $\mathrm{J\,kg^{-1}}$ in order to get the melting water equivalent for that time step.

HESSD
9, 9455–9501, 2012

3.3 Artificial Neural Networks

ANN are approximation methods that imitate the functioning of the human's brain. The brain may be idealized as a high complex non-linear and parallel computer with the capability to perform computations by organizing its neurons and building up its own rules through learning process. In analogy, ANN may reproduce multi variable functions by arranging processing elements (neurons) interconnected according certain rules that may change in order to find the optimal ones (learning). The most popular type of ANN is the Multi Layer Perceptron (MLP).

The MLP configuration consists of interconnected nodes (neurons) arranged into three layers: input layer, a hidden layer and an output layer (Fig. 3). The input layer sends the input vector $\boldsymbol{X}$ of signals x_i to the hidden layer. The hidden layer enables the network to learn by extracting meaningful features from the input. Each neuron process its output y_j by summing its input signal x_i multiplied by its respective weight w_{ij} and a given threshold a_o (Eq. 5).

$$y_j = a_o + \sum x_i w_{ij} \quad (5)$$

The output of each neuron may go to the next hidden layer or to the output node (if only one hidden layer). The main characteristics of a MLP are (a) that each neuron includes a soft non linearity (sigmoidal logistic function which is described in Eq. 6), (b) its layered architecture allows to learn by progressively extracting information from the input, and (c) its high degree of connectivity so that one element of a given layer feeds all the nodes of the next layer.

$$z_j = \frac{1}{1 + \exp(-y_j)} \quad (6)$$

In this study the MLP was trained with the back-propagation algorithm of the software Waikato Environment for Knowledge Analysis (WEKA) version 3.6.6 (Hall et al., 2009).

HESSD
9, 9455–9501, 2012

The performance was evaluated by the non-overlapping test set selection cross validation method, also known as the k-fold method. This is one of the most popular validation methods, and can be described in the following five steps:

1. The total available data n is divided into k non overlapping data subsets $C_1, C_2, \ldots, C_k$, also known as folds.
2. One fold is used for validation, while the remaining folds are used as training data.
3. The created model is tested with the testing fold. This test generates an error E_i.
4. Steps 2 and tree are repeated k times, so that every fold is used once as validation set (Fig. 4).
5. The overall error E is calculated (Eq. 7).

$$E = \frac{1}{k}\sum_{i=1}^{k} E_i \tag{7}$$

While normal hold out testing methods may produce biased results due to the data partitioning, this method gives a much fair and unbiased estimation (Bengio and Grandvelet, 2004). The popularity of the method grew so fast, that studies also compare its performance by using different number of folds. While early ideas suggested using 10 folds, it was found that the differences between 5 and 10 folds are not significant (Uguz and Kodaz, 2011; Iliadis et al., 2011). Markatou et al. (2005) stated that 4 folds is a reasonable number that provides fair estimations. The performance of each model was in terms of correlation coefficient (correlation), mean absolute error (MAE) (Eq. 8), root mean squared error (RMSE) (Eq. 9).

$$\text{MAE} = \frac{1}{n}\sum_{i=1}^{n} |P_i - T_i| \tag{8}$$

$$\mathrm{RMSE} = \sqrt{\frac{1}{n}\sum_{i=1}^{n}\left(\frac{P_i - T_i}{T_i}\right)^2} \tag{9}$$

where

- P_i = predicted value,
- T_i = target value,
- n = total number of samples.

With the SGM estimated for every time step, an ANN was developed in order to estimate SGM using less parameter. The first step was to identify the possible input variables. The data to be used is from a HOBO-U30 data logger that measures short wave incoming radiation, temperature, wind speed and relative humidity. The most important variables are solar radiation and temperature. Also relative humidity was considered to influence the melting process (Kuhn, 1987). In order to reflect the derivative of radiation, temperature and possible freezing effects, data from previous time steps was considered. Since previous ANN studies applied to stage-discharge relations showed that the present discharge is required for determining the discharge at the next level (Bhattacharya and Solomatine, 2000), also the SGM from the previous time step. Previous studies of ANN to hydrologic studies showed that the two antecedent events give better results (Hettiarachchi et al., 2005); thus, data from different previous time steps were considered. The possible inputs considered were current solar radiation (s), solar radiation from a given previous time step i (s_{-i}), current temperature (t), temperature from a given previous time step i (t_{-i}), relative humidity (rh), relative humidity from previous time step i (rh_{-i}), month (m), hour (h) and melting from previous time step i (w_{-i}). Then, ANN with 16 different combinations of the input data were developed. According to the main data used, the models were divided into three groups: (a) considering melting from previous time steps, (b) neglecting relative humidity and previous

Discussion Paper | Discussion Paper | Discussion Paper | Discussion Paper |

HESSD

9, 9455–9501, 2012

Snow glacier melt estimation in tropical Andean glaciers

V. Moya Quiroga et al.

melting, and (c) neglecting previous melt, but considering relative humidity. Each combination was given the name MLP_j, meaning Multi Layer Perceptron and the number of combination j. Table 1 shows the different input combinations used. Table 2 shows the ranges of the used data.

4 Results and discussion

To validate the model, the results were compared with glaciological measurements performed on the glacier (Perroy et al., 2007). Both estimations show a convex pattern with a melting increase between 2003–2004, maximum melting between 2004–2005 and then a decrease between 2005–2006. The energy based estimations are similar to the glaciological measurements, with differences around 200 mm yr^{-1}. The year 2004 has the greatest difference of about 400 mm yr^{-1} (Fig. 5). Analyzing the global radiation trend over the years it can be noticed that 2004 has the highest standard deviation which is about 10–34 % higher than the other years (Table 3). This might have influence in the discrepancies for the melting rates of 2004. It is important to remember that no matter how sophisticated a model is, it aggregates complex properties and processes; as consequence, there are certain parameters that can't be inferred directly, but have to adjusted so that the model approximates as closely as possible to the reality (Vrugt et al., 2012). This classical approach of calibration introduced by Carl Friedrich Gauss in the 18th century is not realistic, as it neglects sources of uncertainty such as data errors or model limitations (Vrugt et al., 2008). Hence, in the last years more realistic methods considering uncertainty began to appear in the literature (Vrugt et al., 2003). Since the main objective of this paper is not to analyse uncertainty (which will be done in a further stage) but to develop a new methodology for simulating SGM rates, the energy balance method is accepted as accurate enough and its rates used as base SGM rate.

Analysing the yearly pattern (Fig. 6), it is possible to note the influence of seasonality, with higher melting during the summer months. The winter months present low melting

HESSD
9, 9455–9501, 2012

rates (around 0.50 mm h^{-1}) which are about one third of the summer rates (between 7 and 8 mm h^{-1}). The daily melting rates (Fig. 7) shows that the melting is limited to day hours between 07:00 and 17:00 (Local time) with some sparse values at 06:00 and 18:00. The daily pattern looks like a Gaussian curve, with its maximum between 11:00 and 12:00.

The obtained results (more than 62 400 time series data) were used for training the 16 MLP models. Performance of each ANN was evaluated by the criteria of correlation (Table 4), mean absolute error (MAE) and root mean squared error Each (RMSE).

The 16 models evaluated were divided into three groups: (a) the ones considering melting from previous time steps (models 1 to 4), (b) the ones neglecting both previous melting and relative humidity (models 5 to 10) and (c) the ones neglecting previous melting but considering relative humidity (models 11 to 16).

The models from the group (a) (Fig. 8) have the highest correlation and the lowest errors. Model 1 considering all the inputs have the best performance. Neglecting relative humidity (model 2) does not have much influence; the correlation deceases 0.003 and the errors increase in 0.03 (MAE) and 0.05 (RMSE). Neglecting one non-physical parameter (month or hour) does not have influence, but neglecting both decreases the correlation in 0.03 (10 times the neglecting of rh).

The models from group b have the lowest correlation and highest errors. This group may be divided into 2 subgroups: (b1) with models 7, 9 and 10 considering only temperature and radiation (Fig. 9) and sub group (b2) with models 5, 6 and 8 also considering the month and hour (Fig. 10). Sub group b1 had the lowest performance with average correlation of 0.56. The consideration of month and hour (sub group b2) increased the performance around 0.07, with an average performance of 0.63.

Including relative humidity increased significantly the performance of the models. This group may be divided into two sub groups: sub group (c1) (Fig. 11) considering only current relative humidity (models 11 and 12) and sub group (c2) (Fig. 12) considering relative humidity from previous time steps (models 13, 14, 15 and 16). Sub group c1 had lower performance with an average correlation of 0.74. The inclusion of

HESSD
9, 9455–9501, 2012

a third previous time step of radiation and temperature (model 12) improved the model correlation from 0.74 to 0.78. The performance of the model was improved by considering relative humidity from previous time steps. Sub group c2 had better performance. Models 13 and 14 considering also month and hour had an average correlation of 0.795. Considering a second previous time step of relative humidity (model 14) almost had no influence, it only made the model more complex with almost the same correlation (little lower) and higher MAE and RMSE, maybe due to an over fitting of the model at some specific points. Neglecting the influence of month decreases the correlation to 0.76 (model 15), and neglecting month and hour (model 16) decreases the correlation to 0.74, a value similar to sub group c1.

The ANN was applied to Condoriri glacier from July 2011 to October 2011, which is the end of winter and the beginning of spring. The estimations began at morning hours when usually there is no melt. In the first time step estimation it was assumed that melting from the two (2) previous time steps was zero (0). The melting from the winter months (July and August) is similar and around 300 mm month^{-1}. The spring months (September and October) show a great increase in the melting to rates around 850 mm month^{-1} and 1050 mm month^{-1} (Fig. 13).

Statistical plots of the daily melting rates for each month (Figs. 14 to 17) shows that the melting process is limited to the daylight hours, with different melting hours and melting rates for each month. In July and August the melting hours are between 08:00–15:00. Although in September most of the melting hours are also from 08:00 to 15:00, there is considerable number of outliers at 07:00 and at 16:00; thus, it could be reasonable to consider that the melting period includes those hours. In October the melting hours are from 07:00 to 17:00; moreover, there are some outliers at 06:00 and a small increase from 18:00 to 19:00.

For an easier understanding of the daily pattern, the melting rates were averaged hourly for each month. The daily pattern (Fig. 18) shows that the highest melting ranges are at noon, and every month there is an increase in the melting hours. In July the highest melting rate of about 0.5 mm h^{-1} is between 10:00 to 14:00, and melting hours are from 06:00 to 16:00 p.m. In August the highest melting rate is little higher than 0.6 mm h^{-1} and is around 13:00. The melting time (from 07:00 to 17:00) is the same and in July (10 h) but a shift of 1 h. The period from August to September has a big increase in the melting, coincident with the season change (From winter to spring). The highest melting rate in September is 1.2 mm h^{-1}, which is twice the previous one; there is also a change in the shape of the curve, with more area toward the late hours; for instance, at 16:00 the September's rate is 0.6 mm h^{-1}, while in July is less than 0.3 mm h^{-1}. In October the highest rate at 12:00 reaches values near 1.4 mm h^{-1}, and from 09:00 to 11:00 there is an almost constant melting rate of 1.2 mm h^{-1}. The total melting time is from 06:00 to 18:00 (12 h).

Detailed analysis from each month (Table 5) shows that July and August have the same mean melting, but the third quartile and the maximum rate from August is 1.8 mm h^{-1} higher and also the third quartile is higher. Thus, August has more time steps with higher melting rate. From August to September the maximum rate has the same increment (1.8 mm h^{-1}), but the third quartile and the mean have much higher increment (0.18 mm h^{-1} and 0.21 mm h^{-1} respectively). This shows that in September there is a much higher number time steps with higher melting rates. In the period from September to October there is also an increment in all the rates.

5 Conclusions

The present research developed ANN models to estimate SGM by the use of simple and easy to obtain data (short wave radiation and temperature) complement with additional easy to obtain inputs. Different combinations were tested ranging from models with only radiation and temperature, to models including relative humidity, month, time and previous melting. Results suggest that only short wave radiation and temperature are not enough to clearly reproduce the melting process at the desired time step. The estimations were highly improved by considering relative humidity from the current and previous time steps. Including melting rate from previous time steps is other input that increases the accuracy, and the most complete model was also the one with the best performance. As any ANN model, is important to consider the ranges of data used in training process. Besides, in the present case is important to note that the highest melting rate predicted is 8 mm h^{-1}. Results with higher rates should be carefully analysed.

The melting from previous time steps has strong influence on improving the global performance and the models of this category had the best performance. The models with the lowest performance were the ones that only considered radiation and temperature. By considering RH the performance could be highly improved. The less relevant data are the ones about non-physical data (month and hour).

The ANN capability to reproduce nonlinear processes allowed estimating SGM at short time steps. The estimation of the Condoriri glacier accurately reproduces the daily and monthly pattern. The monthly SGM at Condoriri begins in the winter month of July coinciding with the lowest rates. The following months present increasing values of the maximum melting rate, the mean rate and the skewness toward higher rates, representing the season change from winter to spring.

The present paper presents a novel methodology for estimating the complex process of SGM at different hours in tropical glaciers using easy to obtain data. Such results reflect the daily pattern of SGM which is very important for the study of tropical glaciers, since the daily variation is greater than the yearly one. These results will provide incoming water into a basin which will be useful for modelling different water scenarios in hybrid basins (glaciological and hydrological). For better understanding of the SGM and the other hydrological processes within the basin, further research will focus on the uncertainty.

Acknowledgements. The authors would like to thank the "Science and Technology Research Partnership for Sustainable Development" (SATREPS) of "Japan Science and Technology Agent – Japan International Cooperation Agency" (JST-JICA). This research is developed within the framework of the GRANDE project, financed by SATREPS

References

Abbott, M. B., Bathurrst, J. C., Cunge, J. A., O'Connell, P. E., and Rasmussen, J.: An introduction to the European Hydrologycal System – Systeme Hydrologique Europeen, "SHE", 2: Structure of a physically based, distributed modelling system, J. Hydrol., 87, 61–77, 1986.

Akhtar, M. K., Corzo, G. A., van Andel, S. J., and Jonoski, A.: River flow forecasting with artificial neural networks using satellite observed precipitation pre-processed with flow length and travel time information: case study of the Ganges river basin, Hydrol. Earth Syst. Sci., 13, 1607–1618, doi:10.5194/hess-13-1607-2009, 2009.

Ambach, W.: Nomographs for the determination of meltwater from snowand ice surfaces, Berichte des naturwissenschaftlich-medizinischen Vereins in Innsbruck, 73, 7–15, 1986.

Anderson, B., Mackintosh, A., Stumm, D., George, L., Kerr, T., Winter-Billington, A., and Fitzsimons, S.: Climate sensitivity of a high-precipitation glacier in New Zealand, J. Glaciol., 56, 114–128, 2010.

Asaoka, Y. and Kominami, Y.: Spatial snowfall distribution in mountainous areas estimated with a snow model and satellite remote sensing, Hydrological Research Letters, 6, 1–6, 2012.

Avian, M. and Bauer, A.: First Results on Monitoring Glacier Dynamics with the Aid of Terrestrial Laser Scanning on Pasterze Glacier (Hohe Tauern, Austria), 8th International Symposium on High Mountain Remote Sensing Cartography, 27–35, 2006.

Bhattacharya, B. and Solomatine, D. P.: Application of artificial neural network in stage-discharge relationship, 4th International Conference on Hydroinformatics, 1–7, 2000.

Bengio, Y. and Grandvelet, Y.: No unbiased estimator of the variance of K-fold cross-validation, J. Mach. Learn. Res., 5, 1089–1105, 2004.

Biggs, T. and Whitaker, T.: Critical elevation zones of snowmelt during peak discharges in a mountain river basin, J. Hydrol., 438–439, 52–65, 2012.

Bocchiola, D., Diolaiuti, G., Soncini, A., Mihalcea, C., Agata, D., Mayer, C., Lambrecht, A., and Rosso, R.: Prediction of future hydrological regimes in poorly gauged high altitude basins: the case study of the upper Indus, Pakistan, Earth, 15, 2059–2075, 2011.

Cobaner, C.: Evapotranspiration estimation by two different neuro-fuzzy inference systems, J. Hydrol., 398, 292–302, 2011.

Coudrain, A., Francou, B., and Kundzewicz, Z.: Glacier shrinkage in the Andes and consequences for water resources Editorial, Hydrolog. Sci. J., 50, 925–932, 2005.

Dai, X., Shi, H., Li, Y., Ouyang, Z., and Huo, Z.: Artificial neural network models for estimating regional reference evapotranspiration based on climate factors, Hydrol. Process., 23, 442–450, 2009.

Debele, B., Srinivasan, R., and Gosain, K.: Comparison of process-based and temperature-index snowmelt modeling in SWAT, Water Resour. Manag., 24, 1065–1088, 2009.

Fu, L., Trudel, M., and Kim, V.: Optimizing winter road maintenance operations under real-time information, Eur. J. Oper. Res., 196, 332–341, 2009.

Hall, M., National, H., Frank, E., Holmes, G., Pfahringer, B., Reutemann, P., and Witten, I.: The WEKA data mining software: an Update, SIGKDD Explorations, 11, 10–18, 2009.

Henneman, H. and Stefan, H.: Albedo models for snow and ice on a freshwater lake, Cold Reg. Sci. Technol., 29, 31–48, 1999.

Hettiarachchi, P., Hall, M. J., and Minns, A. W.: The extrapolation of artificial neural networks for the modelling of rainfall runoff relationships, J. Hydroinform., 7, 2291–296, 2005.

Hirabayashi, Y., Kanae, S., Motoya, K., Masuda, K., and Petra, D.: A 59-year (1948–2006) global meteorological forcing data set for land surface models. Part II: Global snowfall estimation, Hydrological Research Letters, 2, 65–69, 2008.

Hirabayashi, Y., Doll, P., and Kanae, S.: Global-scale modeling of glacier mass balances for water resources assessments: glacier mass changes between 1948 and 2006, J. Hydrol., 390, 245–256, 2010.

Hoai, N. D., Udo, K., and Mano, A.: Using ANN for flood prediction, Journal of Applied Mathematics, 2011, 1–14, 2011.

Hock, R.: A distributed temperature – index ice – and snowmelt model including potential direct solar radiation, J. Glaciol., 45, 101–111, 1999.

Hock, R.: Temperature index melt modelling in mountain areas, J. Hydrol., 282, 104–115, 2003.

Hock, R. and Holmgren, B.: Some aspects of energy balance and ablation of Storglaciaren, Northern Sweden, Geogr. Ann., 78, 121–131, 1996.

Hock, R. and Holmgren, B.: A distributed surface energy-balance model for complex topography and its application to Storglaciaren, Sweden, J. Glaciol., 51, 25–36, 2005.

Hung, N. Q., Babel, M. S., Weesakul, S., and Tripathi, N. K.: An artificial neural network model for rainfall forecasting in Bangkok, Thailand, Hydrol. Earth Syst. Sci., 13, 1413–1425, doi:10.5194/hess-13-1413-2009, 2009.

Huo, Z., Feng, S., Kang, S., Huang, G., Wang, F., and Guo, P.: Integrated neural networks for monthly river flow estimation in arid inland basin of Northwest China, J. Hydrol., 420–421, 159–170, 2012.

Huss, M., Jouvet, G., Farinotti, D., and Bauder, A.: Future high-mountain hydrology: a new parameterization of glacier retreat, Hydrol. Earth Syst. Sci., 14, 815–829, doi:10.5194/hess-14-815-2010, 2010.

Iliadis, L., Maris, F., and Tachos, S.: Soft computing techniques toward modeling the water supplies of Cyprus, Neural Networks, 24, 836–841, 2011.

Jansson, P., Hock, R., and Schneider, T.: The concept of glacier storage: a review, J. Hydrol., 282, 116–129, 2003.

Jost, G., Moore, R., Smith, R., and Gluns, D.: Distributed temperature-index snowmelt modelling for forested catchments, J. Hydrol., 420–421, 87–101, 2012.

King, C.: The relation of temperature to energy, J. Chem. Educ., 82, 861–866, doi:10.1021/ed082p861, 2005.

Kisi, O., Ozkan, C., and Akay, B.: Modeling discharge sediment relationship using neural networks with artificial bee colony algorithm, J. Hydrol., 428–429, 94–103, 2012.

Koboltschnig, G. R. and Schöner, W.: The relevance of glacier melt in the water cycle of the Alps: the example of Austria, Hydrol. Earth Syst. Sci., 15, 2039–2048, doi:10.5194/hess-15-2039-2011, 2011.

Kuhn, M.: Micro-meteorological conditions for snow melt, October, 33, 1–3, 1987.

Lafaysse, M., Hingray, B., Etchevers, P., Martin, E., and Obled, C.: Influence of spatial discretization, underground water storage and glacier melt on a physically-based hydrological model of the Upper Durance River basin, J. Hydrol., 403, 116–129, 2011.

Laurie, N. and Crespo, C.: Deconstructing the best case scenario: lessons from water politics in La Paz-El Alto, Bolivia, Geoforum, 38, 841–854, 2007.

Markatou, M., Tian, H., Biswas, S., and Hripcsak, G.: Analysis of variance of cross-validation estimators of the generalization error, J. Mach. Learn. Res., 6, 1127–1168, 2005.

Mote, P. W. and Kaser, G.: The Shrinking Glaciers of Kilimanjaro: can global warming be blamed? A “poster child” for climate change starves for snow and sublimates, Am. Sci., 95, 318–325, doi:10.1511/2007.66.3752, 2007.

Neal, A. L., Gupta, H. V., Kurc, S. A., and Brooks, P. D.: Modeling moisture fluxes using artificial neural networks: can information extraction overcome data loss?, Hydrol. Earth Syst. Sci., 15, 359–368, doi:10.5194/hess-15-359-2011, 2011.

Olefs, M. and Fischer, A.: Comparative study of technical measures to reduce snow and ice ablation in Alpine glacier ski resorts, Cold Reg. Sci. Technol., 52, 371–384, 2008.
Perroy, E., Mendoza, J., Francisco, R., Garreta, P., Ginot, P., and Fuertes, R.: Mediciones Glaciologicas, Hidrologicas & Meteorologicas Año hidrologico 2006–2007, Tech. report, IRD – IHH – SENAMHI, La Paz, 2007.
Radic, V. and Hock, R.: Regional and global volumes of glaciers derived from statistical upscaling of glacier inventory data, J. Geophys. Res., 115, 1–10, 2010.
Scharffenberg, A. and Fleming, M. J.: Hydrologic Modeling System User's Manual, Davis, CA: US Army Corps of Engineers, August, 2010.
Schulla, J. and Jasper, K.: Model Description WaSiM-ETH, Institute for Atmospheric and Climate Science, Swiss Federal Institute of Technology, Zurich, 2007.
Shamseldin, A. Y.: Artificial neural network model for river flow forecasting in a developing country, J. Hydroinform., 12, 22–35, 2010.
Shiklomanov, I. A. and Rodda, J. C.: World Water Resources at the Beginning of the Twenty-First Century, 1st Edn., UNESCO, Cambridge, 2003.
Sicart, J. E., Wagnon, P., and Ribstein, P.: Atmospheric controls of the heat balance of Zongo Glacier (16S, Bolivia), J. Geophys. Res., 110, 1–17, 2005.
Sicart, J. E., Pierre, R., Bernard, F., Bernard, P., and Condom, T.: Glacier mass balance of tropical Zongo glacier, Bolivia, comparing hydrological and glaciological methods, Global Planet. Change, 59, 27–36, 2007.
Sicart, J. E., Hock, R., and Six, D.: Glacier melt, air temperature, and energy balance in different climates: the Bolivian Tropics, the French Alps, and Northern Sweden, J. Geophys. Res., 113, 1–11, 2008.
Sicart, J. E., Hock, R., Ribstein, P., Litt, M., and Ramirez, E.: Analysis of seasonal variations in mass balance and meltwater discharge of the tropical Zongo Glacier by application of a distributed energy balance model, J. Geophys. Res., 116, 1–18, 2011.
Singh, A. K., Deo, M. C., and Sanil Kumar, V.: Prediction of littoral drift with artificial neural networks, Hydrol. Earth Syst. Sci., 12, 267–275, doi:10.5194/hess-12-267-2008, 2008.
Tahir, A. A., Chevallier, P., Arnaud Y., Neppel, L., and Ahmad, B.: Modeling snowmelt-runoff under climate scenarios in the Hunza River basin, Karakoram Range, Northern Pakistan, J. Hydrol., 409, 104–117, 2011.
Uguz, H. and Kodaz, H.: Classification of internal carotid artery Doppler signals using fuzzy discrete hidden Markov model, Expert Sys. Appl., 38, 7407–7414, 2011.

HESSD
9, 9455–9501, 2012
Snow glacier melt estimation in tropical Andean glaciers
V. Moya Quiroga et al.

Van As, D.: Warming, glacier melt and surface energy budget from weather station observations in the Melville Bay region of Northwest Greenland, J. Glaciol., 57, 208–220, 2011.

Verbunt, M., Gurtz, J., Jasper, K., Lang, H., Warmerdam, P., and Zappa, M.: The hydrological role of snow and glaciers in alpine river basins and their distributed modeling, J. Hydrol., 282, 36–55, 2003.

Vergara, W., Deeb, A. M., Valencia, A. M., Bradley, R. S., Francou, B., Zarzar, A., Grundwaldt, A., and Haeusssling, S. M.: Economic impacts of rapid glacier retreat in the Andes, EOS T. Am. Geophys. Un., 88, 2–4, 2007.

Vrugt, J. A., Gupta, H. V., Bouten, W., and Sorooshian, S.: A shuffled complex evolution metropolis algorithm for optimization and uncertainty assessment of hydrologic model parameters, Water Resour. Res., 39, 1–14, 2003.

Vrugt, J. A., ter Braak, C. J. F., Clark, M. P., Hyman, J. M., and Robinson, B. A.: Treatment of input uncertainty in hydrologic modelling: doing hydrology backwards with Markov Chain Monte Carlo simulation, Water Resour. Res., 44, 1–15, 2008.

Vrugt, J. A., ter Braak, C. J. F., Diks, C. G. H., and Schoups, G.: Hydrologic data assimilation using particle Markov chain Monte Carlo simulation: theory, concepts and applications, Adv. Water Resour., online first: doi:10.1016/j.advwatres.2012.04.002, 2012.

Wang, J., Li, H., and Hao, X.: Responses of snowmelt runoff to climatic change in an inland river basin, Northwestern China, over the past 50 years, Hydrol. Earth Syst. Sci., 14, 1979–1987, doi:10.5194/hess-14-1979-2010, 2010.

Yilmaz, A. G., Imteaz, M. A., and Jenkins, G.: Catchment flow estimation using Artificial Neural Networks in the mountainous Euphrates Basin, J. Hydrol., 410, 134–140, 2011.

Zuzel, J. F. and Cox, L. M., *Relative Importance of Meteorological Variables in Snowmelt*, Water Resour. Res., 11, 174–176, 1975.

HESSD

9, 9455–9501, 2012

Snow glacier melt estimation in tropical Andean glaciers

V. Moya Quiroga et al.

Table 1. Input combinations for the different ANN developed.

Combination	Group	Input data
MLP1	a	m, h, s_{-2}, s_{-1}, s, t_{-2}, t_{-1}, t, w_{-2}, w_{-1}, rh
MLP2	a	m, h, s_{-2}, s_{-1}, s, t_{-2}, t_{-1}, t, w_{-2}, w_{-1}
MLP3	a	m, s_{-2}, s_{-1}, s, t_{-2}, t_{-1}, t, w_{-2}, w_{-1}, rh
MLP4	a	s_{-2}, s_{-1}, s, t_{-2}, t_{-1}, t, w_{-2}, w_{-1}, rh
MLP5	b	m, h, s_{-2}, s_{-1}, s, t_{-2}, t_{-1}, t
MLP6	b	m, s_{-2}, s_{-1}, s, t_{-2}, t_{-1}, t
MLP7	b	s_{-2}, s_{-1}, s, t_{-2}, t_{-1}, t
MLP8	b	h, s_{-2}, s_{-1}, s, t_{-2}, t_{-1}, t
MLP9	b	s_{-1}, s, t_{-1}, t
MLP10	b	s, t
MLP11	c	m, h, s_{-2}, s_{-1}, s, t_{-2}, t_{-1}, t, rh
MLP12	c	m, h, s_{-3}, s_{-2}, s_{-1}, s, t_{-3}, t_{-2}, t_{-1}, t, rh
MLP13	c	m, h, s_{-2}, s_{-1}, s, t_{-2}, t_{-1}, t, rh_{-1}, rh
MLP14	c	m, h, s_{-2}, s_{-1}, s, t_{-2}, t_{-1}, t, rh_{-2}, rh_{-1}, rh
MLP15	c	m, s_{-2}, s_{-1}, s, t_{-2}, t_{-1}, t, rh_{-2}, rh_{-1}, rh
MLP16	c	s_{-2}, s_{-1}, s, t_{-2}, t_{-1}, t, rh_{-2}, rh_{-1}, rh

HESSD
9, 9455–9501, 2012

Snow glacier melt estimation in tropical Andean glaciers

V. Moya Quiroga et al.

HESSD
9, 9455–9501, 2012

Table 2. Statistics of the data used to develop the ANN models.

Data	Maximum	Minimum	Average	Std. deviation
Solar radiation	1452.98	0.00	219.13	325.41
Temperature	12.37	−7.41	0.50	2.57
Relative humidity	100.00	0.00	66.01	30.92
Melting rate	10.12	0.00	0.38	0.93

Table 3. Standard deviation of global radiation for the different years.

Year	Std. Deviation ($W\,m^{-2}$)
2003	241.93
2004	266.50
2005	224.71
2006	212.86
2007	198.35
2008	210.39
2009	209.18

HESSD
9, 9455–9501, 2012

Title Page
Abstract | Introduction
Conclusions | References
Tables | Figures
◀| |▶
◀ ▶
Back | Close
Full Screen / Esc
Printer-friendly Version
Interactive Discussion

Table 4. Performance of the developed ANN.

Model	Group	Hidden nodes	Correlation	MAE	RMSE
MLP1	a	6	0.98	0.10	0.18
MLP2	a	5	0.98	0.13	0.23
MLP3	a	5	0.98	0.15	0.25
MLP4	a	4	0.95	0.18	0.30
MLP5	b	4	0.66	0.45	0.71
MLP6	b	4	0.63	0.48	0.74
MLP8	b	3	0.60	0.50	0.76
MLP7	b	4	0.63	0.47	0.74
MLP9	b	2	0.55	0.51	0.80
MLP10	b	1	0.56	0.50	0.79
MLP11	c	5	0.74	0.39	0.66
MLP12	c	6	0.78	0.39	0.62
MLP13	c	5	0.80	0.28	0.57
MLP14	c	6	0.79	0.43	0.65
MLP15	c	5	0.76	0.45	0.69
MLP16	c	5	0.74	0.46	0.67

HESSD
9, 9455–9501, 2012

Snow glacier melt estimation in tropical Andean glaciers

V. Moya Quiroga et al.

Discussion Paper | Discussion Paper | Discussion Paper | Discussion Paper |

HESSD
9, 9455–9501, 2012

Table 5. Summary of SGM rate at Condoriri for the period July 2011–October 2011.

Minimum	1st Qu	Median	Mean	3rd Qu	Maximum
0.00	0.01	0.05	0.22	0.29	2.55
0.00	0.02	0.05	0.22	0.30	4.36
0.00	0.02	0.05	0.43	0.49	6.17
0.00	0.02	0.15	0.60	0.78	6.64

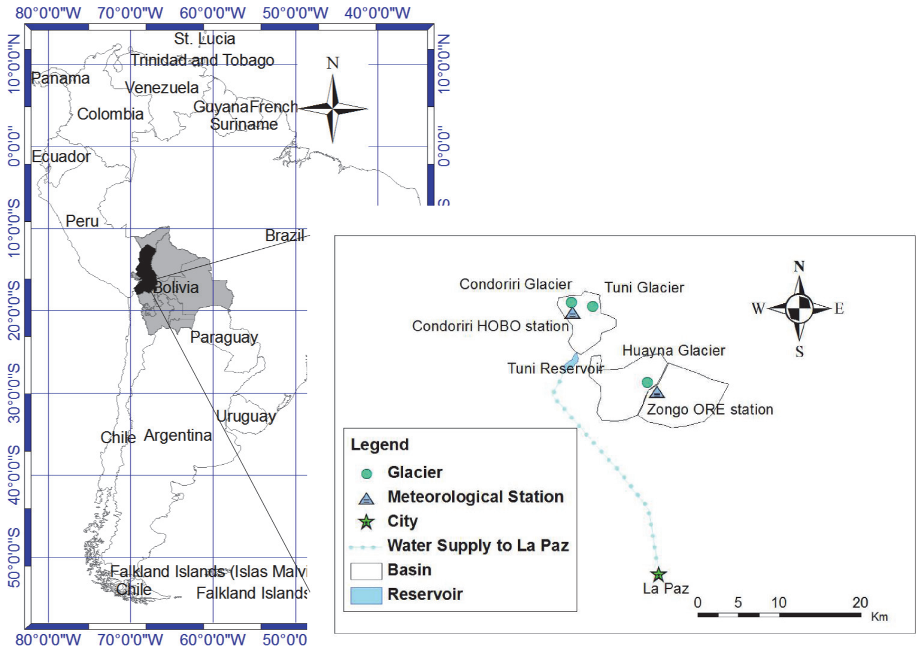

Fig. 1. Location of the study area.

HESSD

9, 9455–9501, 2012

Snow glacier melt estimation in tropical Andean glaciers

V. Moya Quiroga et al.

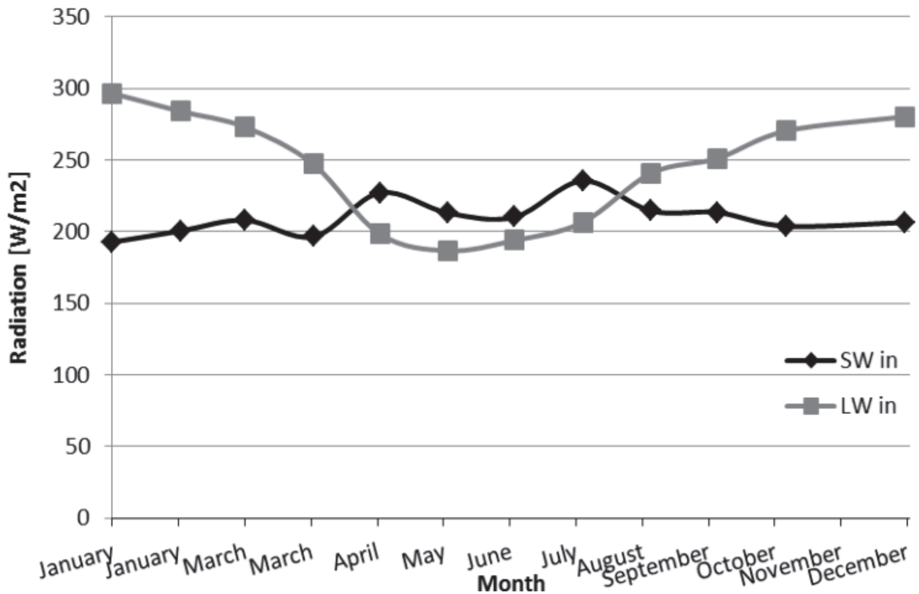

Fig. 2. Yearly variation of incoming short wave radiation (SW_{in}) and incoming long wave radiation (LW_{in}) at the ground surface.

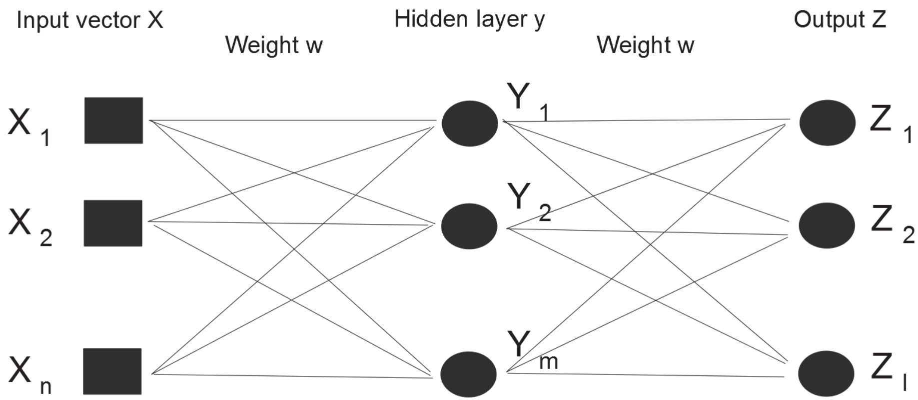

Fig. 3. MLP architecture.

HESSD
9, 9455–9501, 2012

Snow glacier melt estimation in tropical Andean glaciers

V. Moya Quiroga et al.

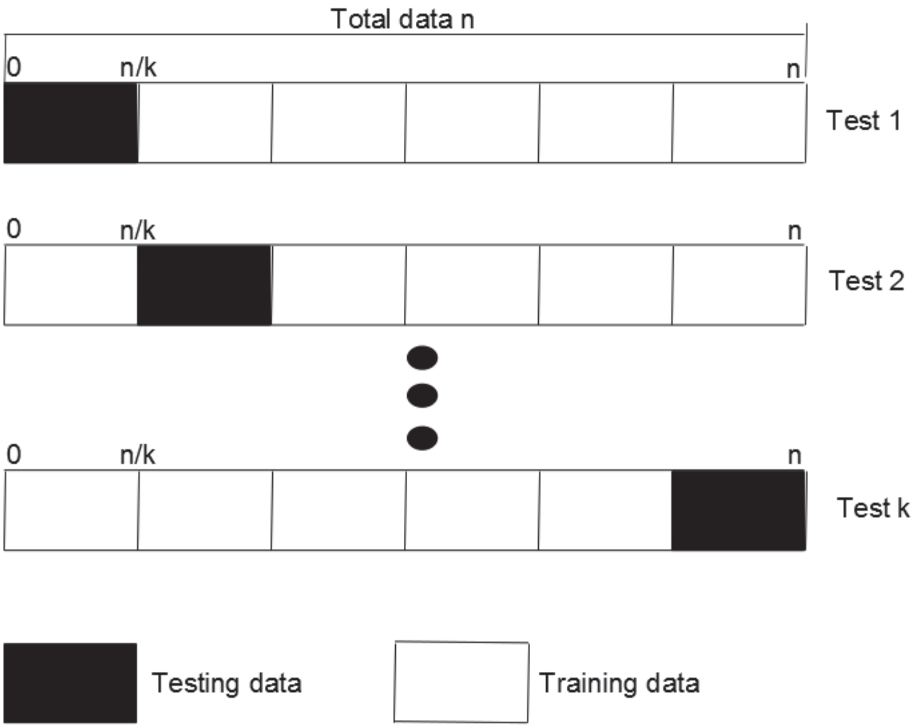

Fig. 4. k-fold cross validation methodology. The total data set is divided into *k* non-overlapping folds. Then, *k* tests are performed using each fold as testing data and the others as training data.

HESSD
9, 9455–9501, 2012

Snow glacier melt estimation in tropical Andean glaciers

V. Moya Quiroga et al.

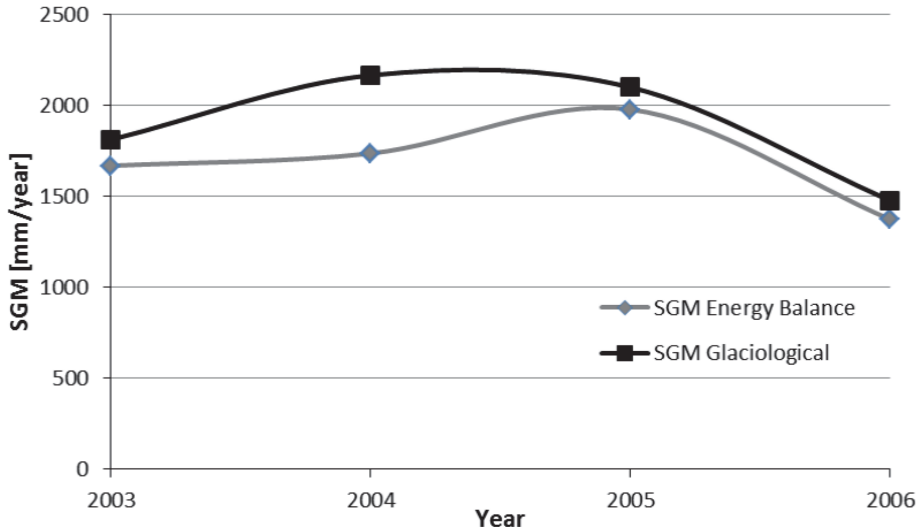

Fig. 5. Comparison of SGM rate estimated by glaciological measurement and SGM estimated by energy balance for the period 2003–2006.

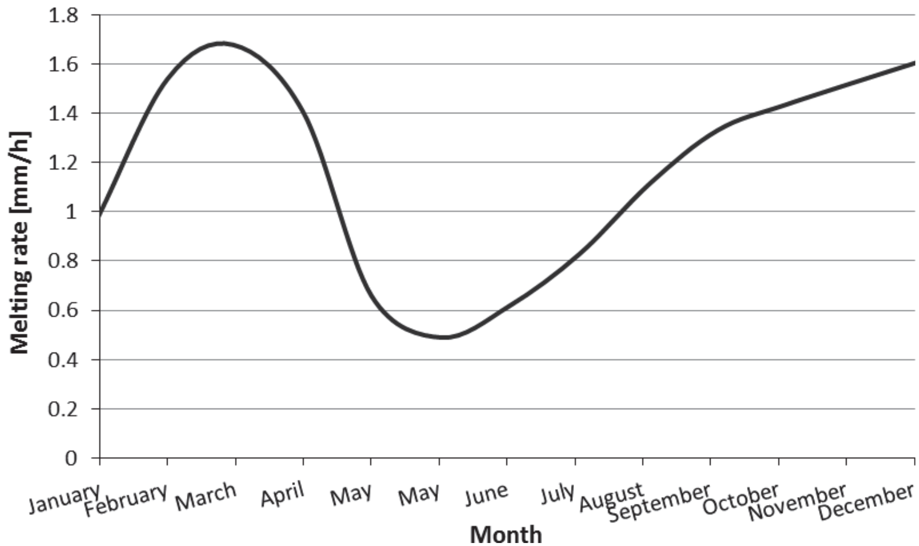

Fig. 6. Monthly average SGM rate throughout the year for the period 2003–2009.

Discussion Paper | Discussion Paper | Discussion Paper | Discussion Paper |

HESSD

9, 9455–9501, 2012

Snow glacier melt estimation in tropical Andean glaciers

V. Moya Quiroga et al.

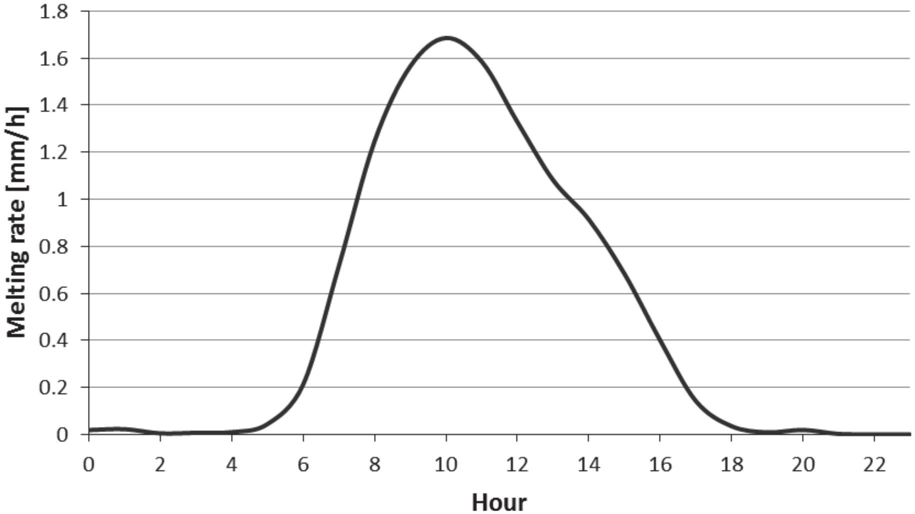

Fig. 7. Daily average SGM rate throughout the day for the period 2003–2009.

HESSD
9, 9455–9501, 2012
Snow glacier melt estimation in tropical Andean glaciers
V. Moya Quiroga et al.

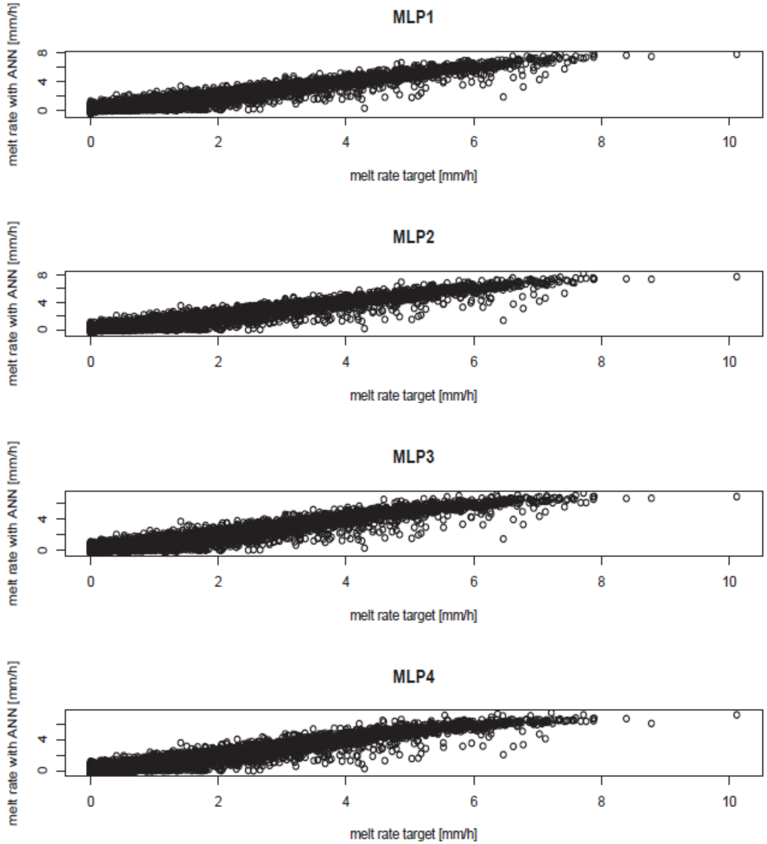

Fig. 8. Scatter plot of SGM rate estimated by energy balance (x-axis) vs. SGM rate estimated by ANN (y-axis) for ANN models of group.

HESSD
9, 9455–9501, 2012

Snow glacier melt estimation in tropical Andean glaciers

V. Moya Quiroga et al.

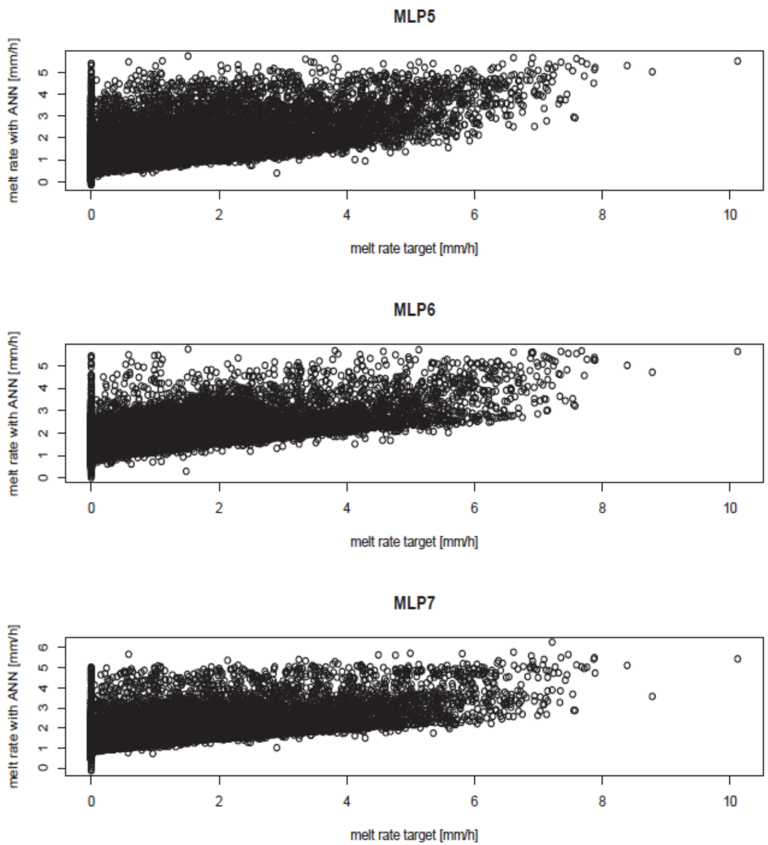

Fig. 9. Scatter plot of SGM rate estimated by energy balance (x-axis) vs. SGM rate estimated by ANN (y-axis) for ANN models of group B1.

HESSD
9, 9455–9501, 2012

Snow glacier melt estimation in tropical Andean glaciers

V. Moya Quiroga et al.

Title Page
Abstract
Introduction
Conclusions
References
Tables
Figures
◀I
▶I
◀
▶
Back
Close
Full Screen / Esc
Printer-friendly Version
Interactive Discussion

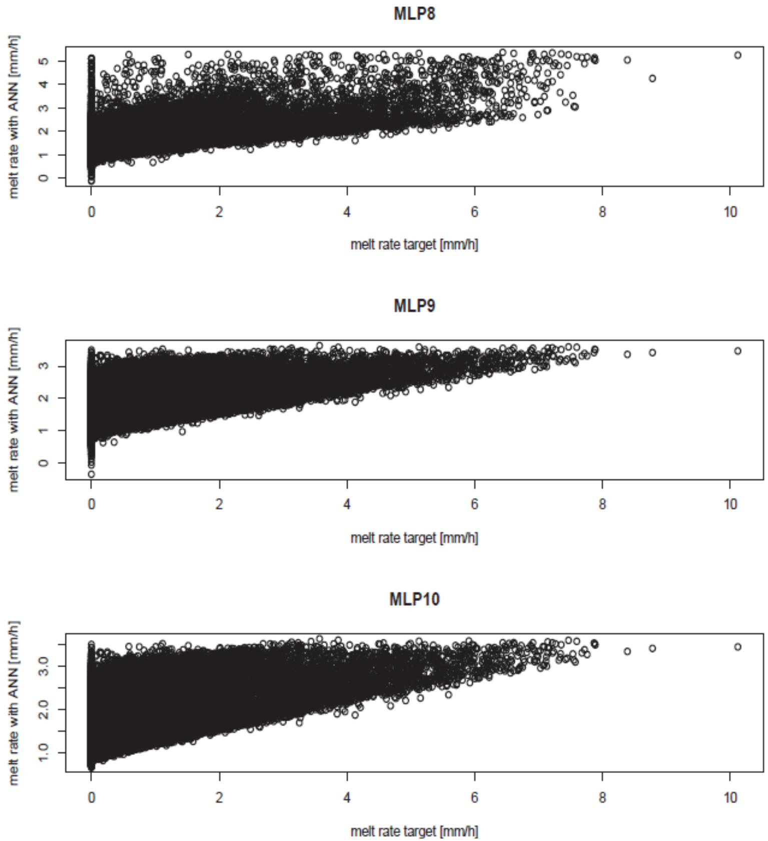

Fig. 10. Scatter plot of SGM rate estimated by energy balance (x-axis) vs. SGM rate estimated by ANN (y-axis) for ANN models of group B2.

HESSD
9, 9455–9501, 2012

Snow glacier melt estimation in tropical Andean glaciers

V. Moya Quiroga et al.

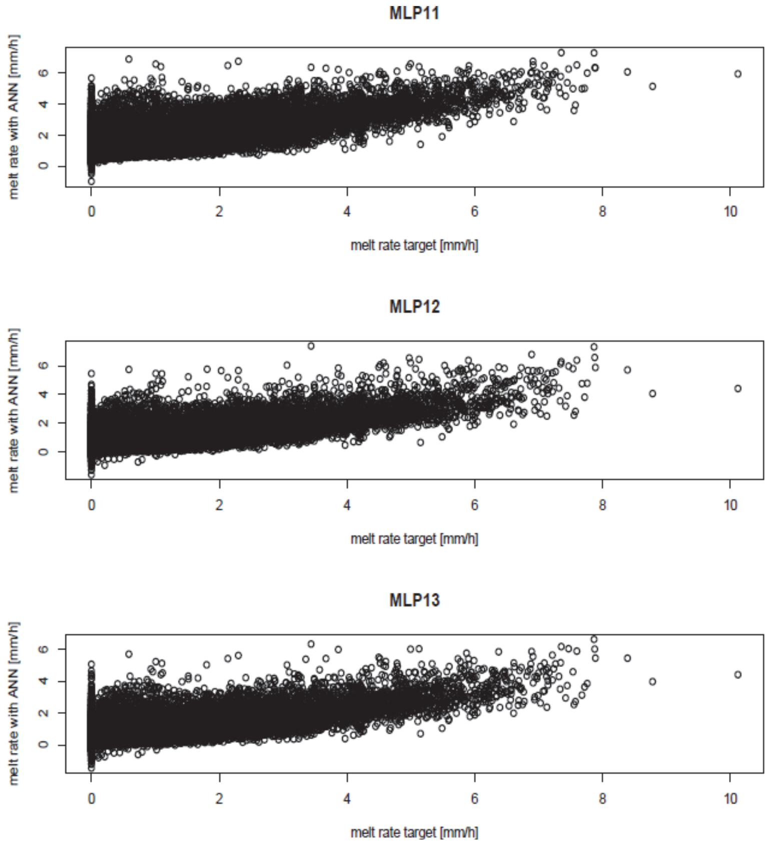

Fig. 11. Scatter plot of SGM rate estimated by energy balance (x-axis) vs. SGM rate estimated by ANN (y-axis) for ANN models of group C1.

HESSD
9, 9455–9501, 2012

Snow glacier melt estimation in tropical Andean glaciers

V. Moya Quiroga et al.

Title Page
Abstract Introduction
Conclusions References
Tables Figures
◀I ▶I
◀ ▶
Back Close
Full Screen / Esc
Printer-friendly Version
Interactive Discussion

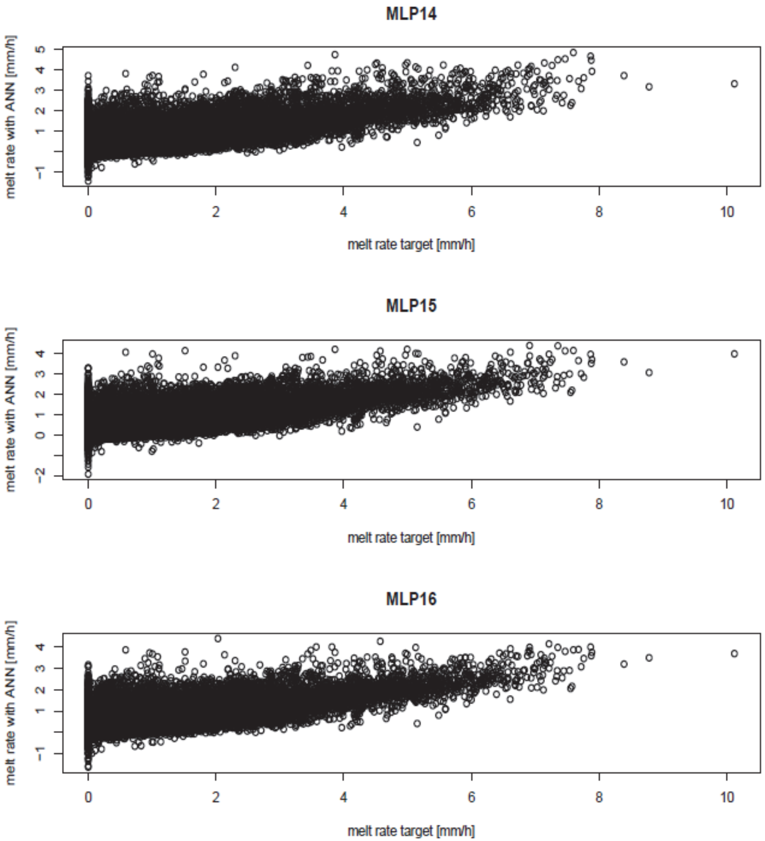

Fig. 12. Scatter plot of SGM rate estimated by energy balance (x-axis) vs. SGM rate estimated by ANN (y-axis) for ANN models of group C2.

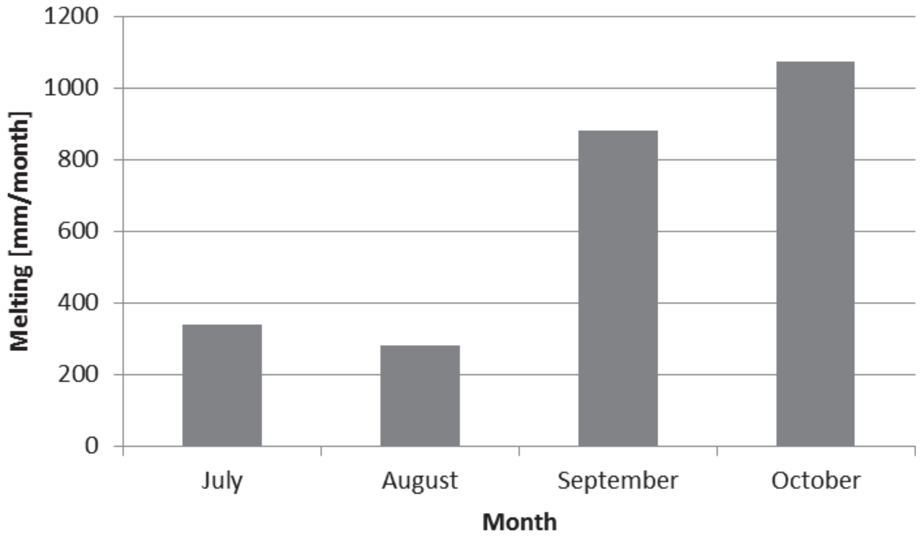

Fig. 13. Monthly SGM rate at Condoriri glacier for the period July 2011–October 2011.

HESSD
9, 9455–9501, 2012

Snow glacier melt estimation in tropical Andean glaciers

V. Moya Quiroga et al.

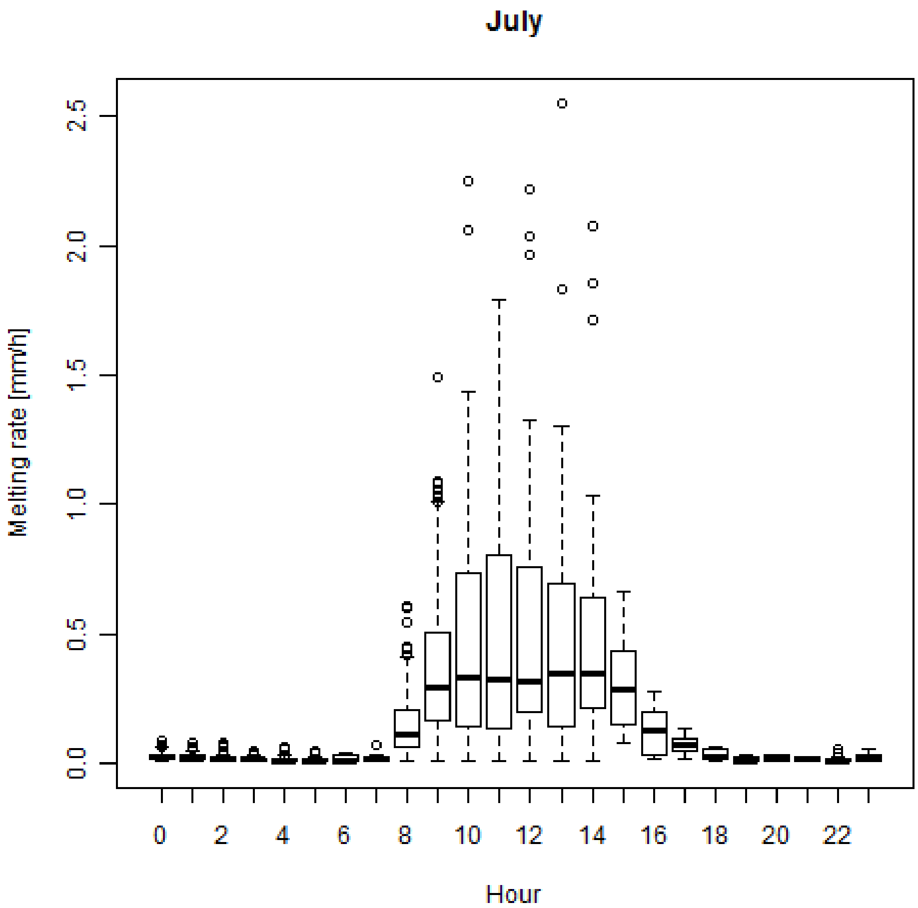

Fig. 14. SGM rate statistics at Condoriri glacier for July 2011. The rectangle represents the rates between the lower and upper quartiles. The black line represents the mean value. The circles represent values that might be considered as outliers.

HESSD
9, 9455–9501, 2012

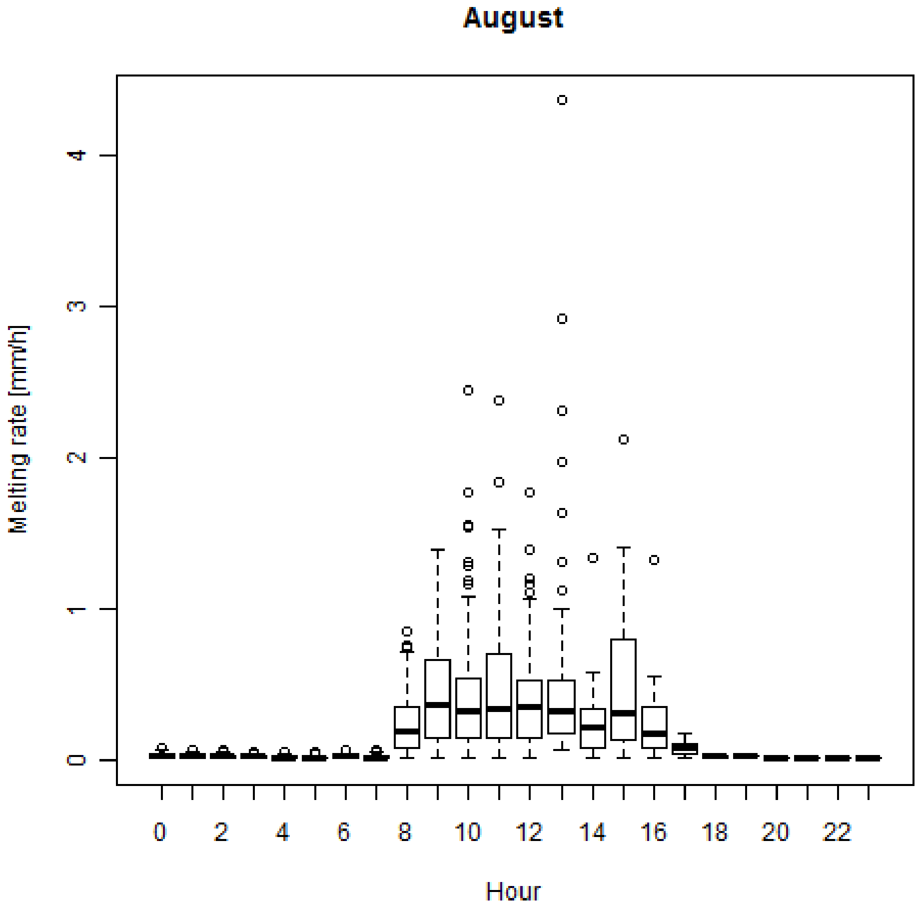

Fig. 15. SGM rate statistics at Condoriri glacier for August 2011. The rectangle represents the rates between the lower and upper quartiles. The black line represents the mean value. The circles represent values that might be considered as outliers.

HESSD
9, 9455–9501, 2012

Snow glacier melt estimation in tropical Andean glaciers

V. Moya Quiroga et al.

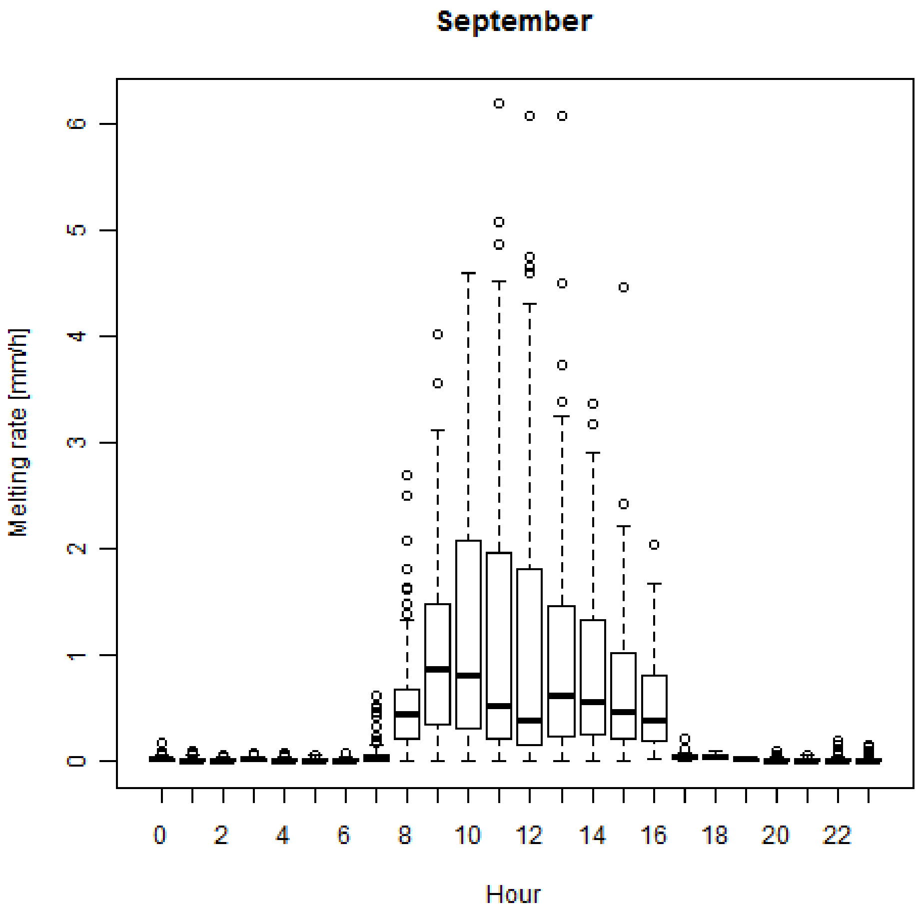

Fig. 16. SGM rate statistics at Condoriri glacier for September 2011. The rectangle represents the rates between the lower and upper quartiles. The black line represents the mean value. The circles represent values that might be considered as outliers.

HESSD
9, 9455–9501, 2012

Snow glacier melt estimation in tropical Andean glaciers

V. Moya Quiroga et al.

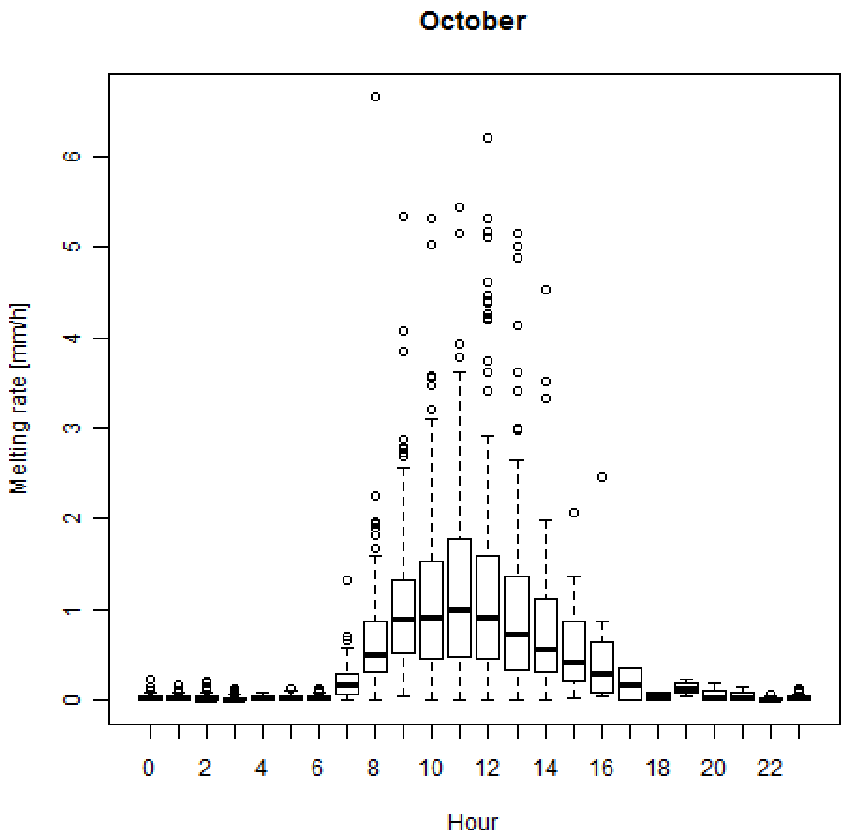

Fig. 17. SGM rate statistics at Condoriri glacier for October 2011. The rectangle represents the rates between the lower and upper quartiles. The black line represents the mean value. The circles represent values that might be considered as outliers.

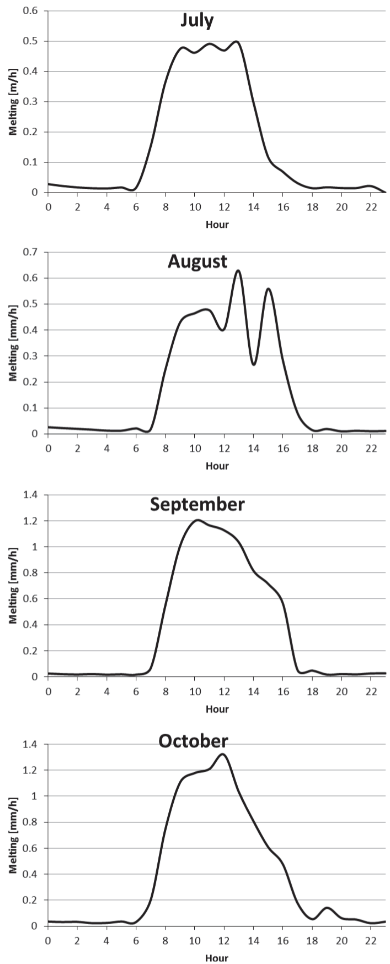

Fig. 18. Hourly SGM rate average at Condoriri glacier for the months July 2011, August 2011, September 2011 and October 2011.

HESSD
9, 9455–9501, 2012